∠CNC is 113°, the conclusion is that, owing to their greater electronegativity, the nitrogens localize the p–π electrons, decreasing the aromatic character of the molecule.

A major point of interest in this analysis of the structure of borazine is the degree of nonplanarity of the molecule. As stated above, both nonplanar models fit the experimental data significantly better than does a rigid D_{3h} model. In Figure 2 it is seen that in the region q = 30–35 the planar model exhibits a slight splitting at the maximum that is not present in either set of experimental data nor in either of the nonplanar models. The resolutions of the electron diffraction photographs and of the microphotometer system are sufficient to show such a feature in the experimental data if it were present.

The calculated shrinkage effect for the two nonplanar models is unusually large. The values obtained are two to four times the comparable value calculated for benzene, as shown in Table IV, and ten times the least-squares standard deviation for N···N. The magnitude of the shrinkage effects leads to the question of whether the observed nonplanarity of the best fitting models is a result of large oscillatory distortions due to vibrational motion.

The choice, then, for the best way to describe the molecular structure of borazine is between a planar D_{3h} model, with exceptionally large out-of-plane vibrational motions such that the probability distribution approaches that for a classical oscillator, and a C_2 model, which is nonpolar in its lowest energy configuration. This choice is not unambiguous, and at this stage, a decision rests on personal preferences. Ultimately the question reduces to one of determining the shape of the potential function of the molecule for out-of-plane distortions. This might be accomplished by a detailed study of the effect of reduced sample temperature on the diffraction patterns. The lowest assigned frequency for borazine (based on D_{3h} symmetry) is 288 cm^{-1}, and the next lowest vibrational frequency is an out-of-plane vibration at 394 cm^{-1}.[28] These correspond to an E_{2u} vibration in benzene, at 404 cm^{-1}, and a B_{2g} vibration at 530 cm^{-1}, indicating considerably lower force constants for distortion from planarity in borazine.

Kubo and his coworkers have calculated simple valence force constants for borazine.[40] However, the recent extensive study of the infrared and Raman spectra[28] of borazine would alter the values of these force constants. A complete normal-coordinate analysis of borazine is expected based on the more recent assignment. It is beyond the scope of this paper to make this normal-coordinate analysis. However, such an analysis must account for the observed nonplanarity of borazine either by assigning a symmetry lower than D_{3h} for the molecule or by indicating the nature of the vibrational motion which results in the observed large shrinkage effects.

Acknowledgments.—This work was supported by the Advanced Research Projects Agency, Army Research Office (Durham), and the National Science Foundation.

(40) H. Watanabe, M. Narisada, T. Nakagawa, and M. Kubo, *Spectrochim. Acta*, **16**, 78 (1960).

CONTRIBUTION FROM THE DEPARTMENT OF CHEMISTRY, CORNELL UNIVERSITY, ITHACA, NEW YORK. 14850

The Molecular Structure of Boroxine, $H_3B_3O_3$, Determined by Electron Diffraction[1]

BY C. H. CHANG, R. F. PORTER, AND S. H. BAUER

Received January 8, 1969

The structure of $H_3B_3O_3$ in the gas phase has been determined by electron diffraction, using digitized microdensitometric data. The heavy atoms are arranged in a planar six-membered ring (D_{3h}). Several nonplanar structures were considered and limits were set on the magnitude of out-of-plane distortion for the average conformation. The bond lengths are B–H = 1.192 ± 0.017 and B–O = 1.3758 ± 0.0021 Å. The bond angles are 120 ± 0.64°.

Introduction

The chemical behavior of boroxine ($H_3B_3O_3$) has been discussed in a series of recent publications.[2,3] The gaseous compound was first observed as one of the products of a high-temperature reaction of H_2 with B–B_2O_3 mixtures.[4] It is also a product in the explosive oxidation of B_2H_6[2] and of B_5H_9.[5] At ambient temperatures, $H_3B_3O_3$ is thermally unstable and decomposes to B_2H_6 and B_2O_3. It has generally been assumed that boroxine is a six-membered heterocyclic ring, similar in structure to borazine ($B_3N_3H_6$). Infrared spectral data may be readily interpreted on the basis of a ring structure.[6]

Since $H_3B_3O_3$ is the simplest member of a large family of boroxine derivatives, it is of importance to define its structure quantitatively. In this paper, we report on

(1) Work supported by the Army Research Office (Durham) and the Advanced Research Projects Agency.

(2) L. Barton, F. A. Grimm, and R. F. Porter, *Inorg. Chem.*, **5**, 2076 (1966).

(3) G. H. Lee, II, and R. F. Porter, *ibid.*, **5**, 1329 (1966).

(4) W. D. Sholette and R. F. Porter, *J. Phys. Chem.*, **67**, 177 (1963).

(5) G. H. Lee, II, W. H. Bauer, and S. E. Wiberley, *ibid.*, **67**, 1742 (1963).

(6) S. K. Wason and R. F. Porter, *ibid.*, **68**, 1443 (1964).

such a determination using electron diffraction techniques.

Experimental Section

Samples of $H_3B_3O_3(g)$ were prepared by initiating with an electrical discharge mild explosions in low-pressure mixtures of diborane and oxygen. The procedure has been described previously.[2] *In these experiments, extreme caution should be exercised since B_2H_6–O_2 mixtures are highly explosive. Reaction vessels should be taped and placed behind a safety shield.* The reaction vessel consisted of a 3-l. round-bottom Pyrex bulb joined to a vacuum stopcock with a 6-in. section of 0.75-in. o.d. Pyrex tubing. The stopcock terminated at a ball joint for attaching the vessel directly to the inlet of the diffraction apparatus. A small piece of Kovar wire sealed in the neck of the bulb served as an electrode for initiating the reaction with a Tesla coil. Mixtures consisting of B_2H_6 and O_2, each at 10 mm pressure, were used throughout these experiments (note precautions in mixing reagents[2]). Under these experimental conditions, the products include $H_3B_3O_3(g)$, hydrogen in a six- to tenfold excess, and solid B_2O_3. The diborane and oxygen are completely consumed. The electron diffraction apparatus has been described earlier.[7] The experimental procedure was to initiate the chemical reaction and then immediately to introduce the sample into the diffraction apparatus through a needle valve. Exposures were always taken within 5 min from the time the sample was prepared. Background pressures within the instrument were below 1.5×10^{-6} mm and the operating pressures were about 5×10^{-5} mm. A cryopump located above the inlet nozzle was lined with FCB activated charcoal to increase its pumping speed for H_2.[8] Diffraction patterns were obtained on 4 × 5 in. Kodak process plates with a 65-kV beam. For q values of 6–68 Å^{-1} and a plate–sample distance of 254.4 mm one preparation of $H_3B_3O_3$ in a 3-l. vessel was adequate for two exposures. For q values 30–136 Å^{-1} and a plate–sample distance of 126.4 mm, one sample of $H_3B_3O_3$ could be used for only one exposure. At each magnification a calibrating exposure with MgO was made. The plates were measured on a double-beam Jarrell-Ash microdensitometer interfaced with a digital recorder. Details of the procedures we followed for data reduction and an error analysis appropriate to our current experimental technique have been described.[9]

Since it was anticipated that diffraction rings from $H_3B_3O_3$ might be masked by excessive scattering from the hydrogen, several preliminary experiments, for calibration purposes, were conducted with hydrogen–benzene mixtures. Table I is a summary of resolution factors obtained from diffraction patterns for a series of H_2–C_6H_6 mixtures. It was found that acceptable diffraction patterns for C_6H_6 can be obtained with mixtures of H_2–C_6H_6 in a molar ratio as high as 9. It was also found that the effect of excess H_2 was reduced considerably when the sample was pumped for about 30 sec before exposing the gas jet to the electron beam.

TABLE I
EXPERIMENTAL RESOLUTION FACTORS

	R_1[a]	R_2[b]	R_3[c]	R_1/R_2	R_2/R_3
Pure C_6H_6	0.6938	0.1098	0.0808	6.32	1.36
C_6H_6–$5H_2$	0.5365	0.0843	0.0604	6.37	1.40
C_6H_6–$9H_2$	0.3448	0.0485	0.0271	7.11	1.79

[a] Resolution factor, $(OD_{max} - OD_{background})/OD_{background}$, at first maximum, q = 19. [b] Resolution factor at second maximum, q = 36. [c] Resolution factor at third maximum, q = 46.

Results

Experimental intensity curves from two sets of diffraction exposures for $H_3B_3O_3$ are shown in Figure 1. Since diffraction from H_2 may contribute to the total intensity at low q values and differences in intensity between maxima and minima were of the same order of magnitude as the experimental uncertainty at angles beyond q = 101, only data from q = 16–54 from set 1 and q = 45–101 of set 2 were used in the analysis. Figure 2 shows the reduced experimental molecular scattering curve, $qM(q)$, and that calculated for the "best" model. (Reduced total intensities at integral q's are listed in Table II.) The refined experimental radial distribution curve and the difference between this and the theoretical curve computed with a damping factor of γ = 0.002287 are given in Figure 3. The first peak in the radial curve is due to the two bonded distances B–H = 1.192 and B–O = 1.376 Å. The second peak with its maximum at 2.36 Å is a superposition of three nonbonded distances, O–H (short) = 2.222 and B–B and O–O = 2.383 Å. Other peaks at 2.75, 3.94, and 3.46 and 4.44 Å are attributed to the nonbonded B–O, O–H (long), B–H, and H–H distances, respectively. In the least-squares calculations with the D_{3h} model, only the l_{ij} values (root-mean amplitude of vibration) for B–H (bonded) and H–H pairs were constrained. The values used were l_{ij}(B–H) = 0.0838 Å, derived from infrared data, and l_{ij}(H–H) = 0.1047 Å, an average from several cycles of the preliminary calculations. All of the other l_{ij} values were allowed to vary. In Table III the converged geometrical parameters are listed, as well as the l_{ij} values for the D_{3h} model. Examination of the error matrix shows that no strong correlations are indicated for the chosen parameters.

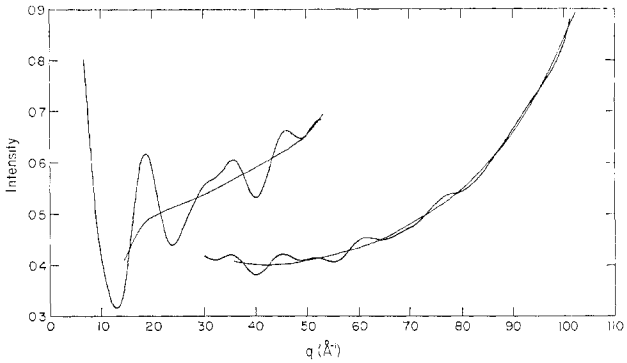

Figure 1.—Experimental intensity curves for $H_3B_3O_3$.

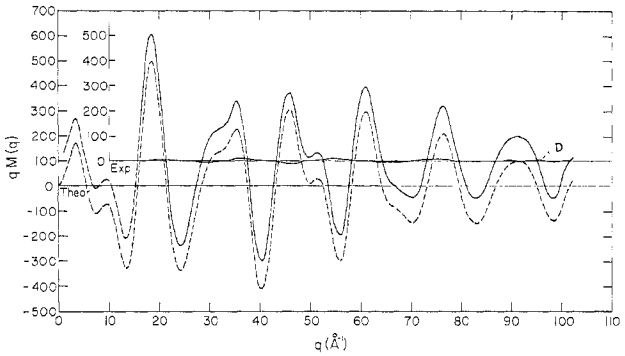

Figure 2.—Experimental and theoretical molecular scattering curves for $H_3B_3O_3$; differences are also shown (curve D).

(7) S. H. Bauer and K. Kimura, *J. Phys. Soc. Japan*, **17**, 300 (1962).
(8) S. H. Bauer and P. Jeffers, *J. Phys. Chem.*, **69**, 3317 (1965).
(9) (a) J. L. Hencher and S. H. Bauer, *J. Am. Chem. Soc.*, **89**, 5527 (1967); (b) W. Harshbarger, *et al.*, *Inorg. Chem.*, **8**, 1683 (1969).

TABLE II

INTENSITY DATA FOR $B_3O_3H_3$

Set 1		Set 2			
Q	INTENSITY	Q	INTENSITY	Q	INTENSITY
8.	0.3761	38.	0.1981	83.	0.3656
9.	0.4898	39.	0.1874	84.	0.3780
10.	0.4228	40.	0.1821	85.	0.3923
11.	0.3653	41.	0.1841	86.	0.4063
12.	0.3271	42.	0.1925	87.	0.4210
13.	0.3153	43.	0.2045	88.	0.4355
14.	0.3310	44.	0.2159	89.	0.4478
15.	0.3836	45.	0.2211	90.	0.4630
16.	0.4669	46.	0.2201	91.	0.4793
17.	0.5543	47.	0.2155	92.	0.4947
18.	0.6132	48.	0.2112	93.	0.5097
19.	0.6174	49.	0.2090	94.	0.5268
20.	0.5796	50.	0.2111	95.	0.5399
21.	0.5258	51.	0.2143	96.	0.5549
22.	0.4789	52.	0.2149	97.	0.5696
23.	0.4505	53.	0.2133	98.	0.5887
24.	0.4419	54.	0.2096	99.	0.6109
25.	0.4519	55.	0.2075	100.	0.6376
26.	0.4710	56.	0.2079	101.	0.6657
27.	0.4978	57.	0.2150		
28.	0.5199	58.	0.2253		
29.	0.5379	59.	0.2378		
30.	0.5532	60.	0.2480		
31.	0.5639	61.	0.2527		
32.	0.5697	62.	0.2529		
33.	0.5778	63.	0.2516		
34.	0.5898	64.	0.2482		
35.	0.6037	65.	0.2492		
36.	0.6057	66.	0.2523		
37.	0.5934	67.	0.2570		
38.	0.5668	68.	0.2626		
39.	0.5410	69.	0.2696		
40.	0.5323	70.	0.2746		
41.	0.5408	71.	0.2812		
42.	0.5668	72.	0.2872		
43.	0.5991	73.	0.2977		
44.	0.6329	74.	0.3084		
45.	0.6554	75.	0.3196		
46.	0.6618	76.	0.3291		
47.	0.6582	77.	0.3346		
48.	0.6495	78.	0.3391		
49.	0.6473	79.	0.3418		
50.	0.6557	80.	0.3444		
51.	0.6692	81.	0.3500		
52.	0.6813	82.	0.3572		

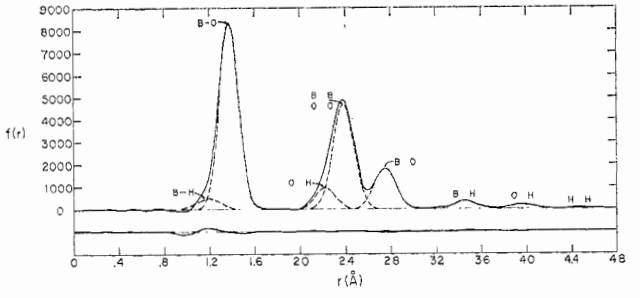

Figure 3.—Refined experimental radial distribution curve for $H_3B_3O_3$ and the difference between this and the theoretical curve for the best model.

Nonplanar models with C_{3v}, C_2, and C_s symmetries were considered in detail. The departure of these configurations from the D_{3h} model is defined by an out-of-plane angle, δ, as illustrated in Figure 4. For each model a least-squares analysis was performed by constraining δ to selected values from 0 to 8°. Converged results for models with small δ angles are given in Table III. In this sequence the l_{ij} values for O–H (short), O–H (long), B–H, and H–H were fixed at 0.0594, 0.0838, 0.0838, and 0.1047 Å, respectively, as deduced in trial calculations. Figure 5 consists of plots of the standard deviations obtained for each model as a function of δ.

Discussion

The cyclic structure of boroxine has been proven in this study; the diffraction data favor D_{3h} symmetry.

TABLE III

RESULTS OF LEAST-SQUARES ANALYSES OF DIFFRACTION DATA FOR GASEOUS $H_3B_3O_3$

	Model									
	D_{3h}	C_{3v}		C_2		C_s				
Parameter[a]	δ = 0.0°	δ = 1°	δ = 3°	δ = 1°	δ = 3°	δ = 1°		δ = 3°		
r_{B-H}	1.1915 ± 0.0042	1.1918 ± 0.0042	1.1937 ± 0.0042	1.1919 ± 0.0042	1.1945 ± 0.0047	1.1917 ± 0.0042		1.1924 ± 0.0043		
r_{B-O}	1.3758 ± 0.0003	1.3756 ± 0.0003	1.3746 ± 0.0003	1.3756 ± 0.0003	1.3744 ± 0.0004	1.3780 ± 0.0003		1.3787 ± 0.0003		
0.5 ∠OBO	1.0472 ± 0.0016	1.0523 ± 0.0016	1.0559 ± 0.0016	1.0525 ± 0.0016	1.0574 ± 0.0018	1.0520 ± 0.0016		1.0537 ± 0.0016		
$l_{B\cdots O}$	0.0646 ± 0.0016	0.0646 ± 0.0016	0.0647 ± 0.0017	0.0647 ± 0.0016	0.0652 ± 0.0018	0.0646 ± 0.0016		0.0647 ± 0.0016		
l_{H-O}	0.0493 ± 0.0003	0.0493 ± 0.0003	0.0493 ± 0.0003	0.0493 ± 0.0003	0.0492 ± 0.0004	0.0492 ± 0.0003		0.0492 ± 0.0003		
$l_{O\cdots O}$	0.0660 ± 0.0007	0.0659 ± 0.0007	0.0652 ± 0.0008	0.0659 ± 0.0007	0.0650 ± 0.0009	0.0659 ± 0.0007		0.0657 ± 0.0007		
$l_{B\cdots B}$										
$l_{O\cdots H(short)}$	0.0594 ± 0.0041									
$l_{O\cdots H(long)}$	0.0838 ± 0.0085									
$l_{B\cdots H}$	0.0838 ± 0.0085									
Std dev	0.02345	0.02349	0.02421	0.02358	0.02646	0.02348		0.02401		
Residual	0.04540	0.04557	0.04849	0.04590	0.05813	0.04553		0.04763		
Error	0.04540	0.04557	0.04849	0.04590	0.05813	0.04553		0.04763		

[a] All distances are in ångströms and the angle is in radians.

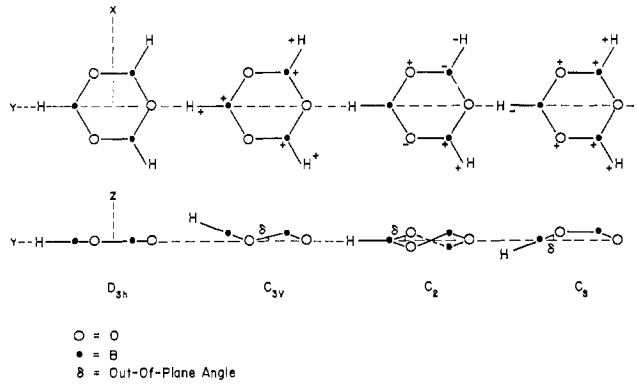

Figure 4.—Models considered in the structure analysis of $H_3B_3O_3$.

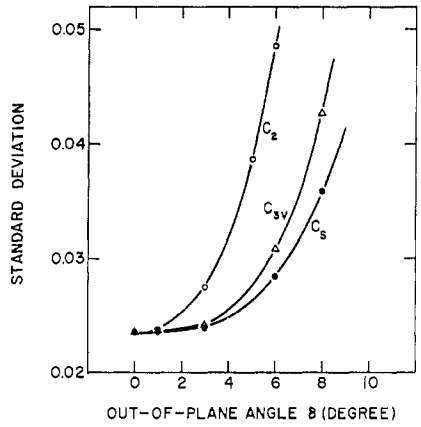

Figure 5.—Plots of standard deviations from least-squares analyses of nonplanar $H_3B_3O_3$ models as a function of the out-of-plane angle δ.

Error limits were assigned as the higher of the estimated magnitudes of systematic errors[9b] or as four times the calculated standard deviations. Therefore the final geometric parameters are B–H = 1.192 ± 0.017 Å, r_{B-O} = 1.3758 ± 0.0021 Å, and ∠BOB = ∠OBO = 120.00 ± 0.64°. The least-squares analyses (Figure 5) show that the standard deviations for nonplanar models converged to a minimum for $\delta = 0$. From these results the maximum uncertainty for the out-of-plane angle δ is estimated to be within 5°. Planar models with nonhexagonal ring angles were examined in trial analyses. However, the radial distribution curve shows that the nonbonded O–O and B–B distances are equal to well within the limits of resolution, consistent with a nearly hexagonal structure.

The magnitude of "shrinkage" of nonbonded B···O due to thermal motion was calculated from[10]

$$-\delta_{B\cdots O} = \left(r_{B\cdots O} + \frac{l_{B\cdots O}^2}{r_{B\cdots O}}\right) - 2\left(r_{B-O} + \frac{l_{B-O}^2}{r_{B-O}}\right)$$

where $r_{B\cdots O}$ = 2.7515 and $l_{B\cdots O}$ = 0.0660 Å are the converged values from a least-squares run of a C_2 model in which B–O, B–H, B···B, and O···O were inserted as independent parameters, whereas r_{B-O} = 1.3758 and l_{B-O} = 0.0493 Å were taken from the D_{3h} model. The small value of $\delta_{B\cdots O}$ (0.0001 Å) is an indication of the high rigidity of the boroxine ring.

(10) W. V. F. Brooks, B. N. Cyvin, S. J. Cyvin, P. C. Kvande, and E. Meisingseth, *Acta Chem. Scand.*, **17**, 345 (1963).

Bond parameters for $H_3B_3O_3$ may be compared with those for two related molecules—$H_2B_2O_3$(g) and the isoelectronic analog, borazine ($H_6B_3N_3$). $H_2B_2O_3$, a product of the reaction of O_2 with boroxine, has the planar cyclic structure

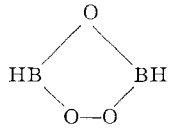

as determined by microwave studies.[11] The two B–O distances are $r_{B-O(apex)}$ = 1.380 ± 0.003 Å and $r_{B-O(base)}$ = 1.365 ± 0.004 Å. The magnitude of r_{B-O} = 1.3758 ± 0.0021 Å in boroxine is intermediate between these values. The bond angles reported for $H_2B_2O_3$ are ∠OBO = 113° 3′, ∠BOB = 104° 0′ and ∠BOO = 104° 57′. Comparison with $H_3B_3O_3$ shows that considerable variation in ring angles is possible in the B–O cyclic systems. From simple bond-hybridization considerations it is difficult to explain the total planarity of these molecules since the ring angles in $H_2B_2O_3$ average close to tetrahedral (sp^3) while the angles in $H_3B_3O_3$ are close to trigonal (sp^2). However, owing to the highly polar nature of the B^+–O^- bond, it is possible that planarity is stabilized by ionic forces resulting from the alternation of positive and negative charges in the ring, by analogy with the calculated minimum energy configuration for $(LiF)_3$, reported by Milne and Cubicciotti.[12]

Comparison of the structural parameters for borazine[9b] with those obtained in this study for boroxine indicate that borazine is considerably less rigid. Since planar stabilization through π bonding should be greater in borazine, this factor cannot account for the difference in the ease of out-of-plane distortion. However, planar stabilization through ionic interactions is probably greater in boroxine, and this may be the more significant factor. In the infrared spectra of borazine and boroxine the B–H asymmetric stretches (E′ type of vibration) are 2520[6] and 2620 cm^{-1},[13] respectively. The lower frequency in borazine reflects the longer B–H bond length.

The B–O bond length in $H_3B_3O_3$ does not appear to be unique since it is within experimental error of 1.373 ± 0.007 Å, reported for the ring B–O distance in solid $(HO)_3B_3O_3$ (metaboric acid);[14] 1.39 ± 0.02 Å, in the trimethyl derivative of boroxine;[15] and 1.38 ± 0.02 Å, in the noncyclic compound trimethyl borate.[15]

Finally, it is now possible to compare the dimensions of four isoelectronic six-member ring molecules which are characterized by different nuclear charge distributions. Note the consequence of the conversion of C_6H_6 [C–C = 1.397 Å] to $H_3C_3N_3$ by uniting the nuclei of alternate CH groups. The ring shrinks by 0.059 Å [C–N = 1.338 Å]. Qualitatively, this effect is a direct con-

(11) W. V. F. Brooks, C. C. Costain, and R. F. Porter, *J. Chem. Phys.*, **47**, 4186 (1967).

(12) T. A. Milne and D. D. Cubicciotti, *ibid.*, **30**, 1625 (1959).

(13) K. Niedenzu, W. Sawodny, H. Watanabe, J. W. Dawson, T. Totanis, and W. Weber, *Inorg. Chem.*, **6**, 8 (1967).

(14) C. R. Peters and M. E. Milberg, *Acta Cryst.*, **17**, 229 (1964).

(15) S. H. Bauer and J. Y. Beach, *J. Am. Chem. Soc.*, **63**, 1394 (1941).

sequence of the increased electron density in the inner ring due to the increase of nuclear charge. The comparable shift of positive charge from the outer to the inner ring of atoms, in the transformation of borazine to boroxine, due to replacement of alternate N–H by O atoms, also leads to a contraction [B–N = 1.435 Å to B–O = 1.376 Å] by exactly the same magnitude, 0.059 Å. However, a redistribution of charge within the ring has the opposite effect. One may imagine the conversion of benzene to borazine by the transfer of protons from alternate carbons to their neighbors. The ring expands by 0.038 Å on a side. The similar nuclear transformation from $H_3C_3N_3$ to $H_3B_3O_3$ has the identical effect. The increase in bond polarity within the rings and associated lowering of the π-electron delocalization by the increase in positive charge at three centers reduce the bond order. A quantitative analysis of the changes in ring dimensions and internal angles remains a worthwhile undertaking.

Acknowledgment.—The authors wish to thank W. Harshbarger, R. Hilderbrandt, M. Cardillo, and J. Chiang for technical assistance and helpful discussions. This work was supported by the Army Research Office (Durham) and the Advanced Research Projects Agency.

CONTRIBUTION FROM THE DEPARTMENT OF CHEMISTRY, UNIVERSITY OF SOUTH DAKOTA, VERMILLION, SOUTH DAKOTA 57069

Borane Cations of Base Oxides

BY N. E. MILLER

Received February 20, 1969

A new class of borane cations with mixed bases is presented containing the oxide bases pyridine N-oxide, trimethylamine N-oxide, trimethylphosphine oxide, and dimethyl sulfoxide. These cations are considerably less stable toward basic hydrolysis than the corresponding cations without oxygen.

It is becoming increasingly clear that the $(base)BH_2^+$ grouping is a strong acid toward a variety of base sites. A striking example was recently presented in the synthesis of $H_2B(base)_2^+$ borane cations with amides bonded through the oxygen of the amide base.[1] Because of the unexpected stability of the cations with weak amide bases, exploration for cations with oxide bases was made and a new class of cations was demonstrated, namely, $(CH_3)_3NBH_2O(base)^+$ where the base is pyridine, trimethylamine, trimethylphosphine, or dimethyl sulfide.

Experimental Section

Practical grade pyridine oxide was rendered anhydrous by sublimation under vacuum at 70°. Trimethylphosphine oxide was prepared from phosphorus oxychloride and methylmagnesium chloride in ether by the method of Burg and McKee.[2] Trimethylamine oxide was prepared according to the method of Hickinbottom.[3] Dimethyl sulfoxide of commercial reagent grade quality was employed without additional purification. Trimethylamine–iodoborane was prepared from iodine and trimethylamine–borane in benzene by the method outlined by Ryschkewitsch and Garrett.[4] Anhydrous chloroform was obtained by distillation from phosphoric anhydride.

Preparation of Cations.—An equimolar amount of trimethylamine–iodoborane in anhydrous chloroform was added rapidly *via* syringe to a solution of the base oxide in chloroform. First contact of the solutions produced an orange coloration that persisted after completion of the addition with all the base oxides but trimethylamine N-oxide. The coloration instantly faded on contact of the solution with air. Solvent was removed after about 1 hr of standing, and the residues were taken up in water. Saturated ammonium hexafluorophosphate solution was added, precipitating the borane cations as the hexafluorophosphate salts. The hexafluorophosphates were recrystallized from acidified hot (about 60–90°) water. Yields were better than 80%.

Rapid handling of the salts of the cation with dimethyl sulfoxide base was required since the iodide and the crude hexafluorophosphate turned a dark orange and softened when left in contact with air. This behavior appears to be a decomposition reaction that probably involves oxygen and is catalyzed by the iodide ion. Recrystallized hexafluorophosphate salt left in the open for days did not discolor, but it slowly decomposed, releasing dimethyl sulfoxide.

Analyses and spectral data for recrystallized samples are collected in Tables I and II.

Hydrolysis.—The hydrolysis apparatus was a 15-ml flask, with a magnetic stirring bar, that was attached to a small gas buret.[5] A 3–10-mg sample of salt was dissolved in a precise quantity of 1.00 *M* potassium chloride contained in a 10-ml volumetric flask. The requisite amount of 1.00 *M* sodium hydroxide was added, the volume was adjusted to 10.0 ml, and the solution was transferred to the reaction vessel along with a small amount of powdered borosilicate glass. Rapid stirring in the presence of the powdered glass ensured uniform gas evolution. Graphical analysis of the data ($V_\infty - V_t$ *vs.* time) yielded the pseudo-first-order rate constants.

All of the borane cations in solution were rapidly degraded by strong base somewhere between room temperature and 100°.

(1) N. E. Miller, D. L. Reznicek, R. J. Rowatt, and K. R. Lundberg, *Inorg. Chem.*, **8**, 862 (1969).

(2) A. B. Burg and W. E. McKee, *J. Am. Chem. Soc.*, **78**, 4590 (1951). Attempts were made to use methylmagnesium bromide as the Grignard reagent with no success. Yields similar to those reported were obtained with methylmagnesium chloride.

(3) W. J. Hickinbottom "Reactions of Organic Compounds," John Wiley & Sons, Inc., New York, N. Y., 1962, p 420.

(4) G. E. Ryschkewitsch and J. M. Garrett, *J. Am. Chem. Soc.*, **89**, 4240 (1967).

(5) A detailed description of the technique is to be published in relation to the hydrolysis of another borane cation.